Control Strategies of Doubly Fed Induction Generators to Support Grid Voltage

M. B. C. Salles[1], J. R. Cardoso[1], A. P. Grilo[2], C. Rahmann[3], K. Hameyer[4]
[1]Laboratory of Applied Electromagnetism - LMAG, University of São Paulo, Brazil
[2]Engineering, Modeling and Applied Social Science Center - Federal University of ABC
[3]Institute of Power Systems and Power Economics - IAEW, RWTH Aachen University, Germany
[4]Institute of Electrical Machines - IEM, RWTH Aachen University, Germany
mausalles@pea.usp.br

***Abstract*- The use of wind power has been increasing very fast in the last 10 years. Many new projects for the next 10 years including offshore and onshore wind farms are been developed and planned. The fast growing of the use of wind power has brought new challenges to the Transmission System Operators (TSO) in regions where wind power has reached significant penetration levels like Denmark, United Kingdom, Spain and Germany. According to new grid code requirements wind turbines must remain connected to the grid during grid disturbances and, moreover, they must also contribute to voltage support during and after grid faults. Dynamic models of doubly fed induction generator (DFIG) were developed to investigate the behavior off different converter control and protection strategies of the back-to-back IGBT-based converters during grid fault. The results have showed that reactive power injection by DFIG-based wind farms is limited when the rotor side converter is blocked.**

***Index Terms*— doubly fed induction generator, induction generator, reactive power control, wind power generation.**

I. INTRODUCTION

A wind turbine (WT) equipped with blade pitch angle control can generate more than 600 KW and are grouped in wind farms from about 40 MW to more than 150 MW in offshore installations. In 2005, 45% of the medium-large wind turbines installed in Europe were based on doubly-fed induction generators (DFIG) [1]. The fact that the penetration level of wind power has increased rapidly in some countries (like Spain, Germany, Denmark and UK) has demanded new abilities from wind power plants to guarantee efficient and reliable operation of the power system. The new grid codes require the ability from wind turbines to keep connected during and after grid faults [2],[3]. More strict grid codes also require the ability to provide voltage support [4],[5] at the same time.

Different from the classical synchronous generator (SG) directly connected to the power system, DFIG-based wind turbines are connected with the use of two back-to-back converters. The control of terminal voltage (or power factor) for the classical SG is by the field excitation, while for the DFIG is by the rotor side converter (RSC) and it is possible also by the grid side converter (GSC). The investigation presented in this paper analyzes different converter control and protection strategies in order to verify the accomplishment of new grid code requirements.

This paper is organized as follows. Section II shortly discusses the dynamic model of the wind turbine. Section III presents the DFIG. In Section IV, the German and the Spanish grid code requirements are discussed. The single line diagram of the test system is shown in Section V. The analyses of the converter control and the protection strategies are presented in Section VI and VII, respectively. The conclusions are discussed in Section VIII.

II. WIND TURBINE DYNAMIC MODEL

Mechanical power capture from the wind can be calculated using the well-know aerodynamic equation [6],[7]:

$$P_m = \frac{1}{2} A \rho V^3 C_P(\lambda, \beta) \tag{1}$$

where A is the turbine rotor area, ρ is the density of the air, V is the wind speed, C_p is the performance coefficient, β is the blade pitch angle, $\lambda = \omega R/V$ is the tip speed ratio, R is the radius of the rotor and ω is the mechanical angular speed of the blades.

The implemented wind turbine model has the performance coefficient modelled by equations (2) and (3), suggested by Hier and optimised by Slootweg [6]. This coefficient indicates how efficient the wind turbine can capture the energy from the wind. The Betz limit is the maximum theoretic value that the *Cp* can reach (0,59 for 3 blades wind turbine [7]). The *Cp* characteristics are experimentally obtained by the manufactures and depend also on the tip speed ratio and on the blade pitch angle values.

$$C_P(\lambda, \beta) = c_1 \cdot \left(\frac{c_2}{\lambda_i} - c_3 \cdot \beta - c_4 \cdot \beta^{c_5} - c_6 \right) \cdot e^{-\frac{c_7}{\lambda_i}} \tag{2}$$

$$\lambda_i = \frac{1}{\frac{1}{\lambda + c_8 \cdot \beta} - \frac{c_9}{\beta^3 + 1}} \tag{3}$$

The values of c1-c9 (reproduced in Table 1) were adapted from the values suggested by Hier in order to better represent the aerodynamics of modern wind turbines [6]. Modern wind turbines have a higher maximum value of the *Cp* for 0º (zero degree) of the blade pitch angle when comparing with old 3 blades wind turbine designs (not shown).

Table 1 Optimized values of the *Cp* curve equations.

c_1	c_2	c_3	c_4	c_5	c_6	c_7	c_8	c_9
0,73	151	0,58	0,002	2,14	13,2	18,4	-0,02	-0,003

The Cp curves implemented in these studies were calculated by equation (2) and (3) and they are shown in Fig. 1.

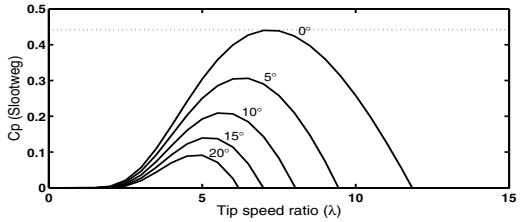

Fig. 1 Cp curves suggested by Slootweg for different pitch angle position.

III. Doubly-Fed Induction Generator (DFIG)

This is the most wide spread configuration of wind turbine since the development of highly efficient power electronics [1]. This concept consists in two back-to-back voltage source converters connecting the grid and the rotor windings. Stator circuits are connected direct to the grid (Fig. 2). The parameters of the DFIG used in this analysis can be found in [6]. The rotor-side converter control complemented by the pitch angle control regulates the electric power to its optimum value to maximize the *Cp* during operation.

A. Control of the Rotor-Side Converter (RSC)

In normal operation, rotor-side converter regulates the reactive power injection and the developed electric power (P_{elec}). The optimum electric power reference (P^*_{opt}) is calculated taking into account the optimal rotor speed for the incoming wind considering the *Cp* curves (Fig. 1). In Fig. 3, the control used in the simulations is shown. The encoder gives the generator rotor position (θ) to the abc-dq0 and to the dq0-abc transformations. The direct axis component is used to regulate the generator power factor to 1 pu thus, the absorbed reactive power reference (Q^*) is equal to 0 (zero). The quadrature axis component is controlled similarly to the direct axis, however, it regulates the electric power to the P^*_{opt}. After a dq0-to-abc transformation, V^*d and V^*q are sent to the PWM (Pulse-width Modulation) signal generator. Finally, V^*abcr are the three-phase voltages desired at RSC output.

B. Control of the Grid-Side Converter (GSC)

In normal operation, the voltage of the DC-link between RSC and GSC is controlled by the GSC (Fig. 4). Such controller employs a PLL (Phase Locked Loop) providing the angle (ϕ) to the abc-to-dq0 (and dq0-to-abc) transformation to synchronize the three-phase voltages at the converter output with the zero crossings of the fundamental component of the phase-A of the terminal voltage. The direct axis component is used to regulate DC link voltage (V^*dc) to 1 pu.

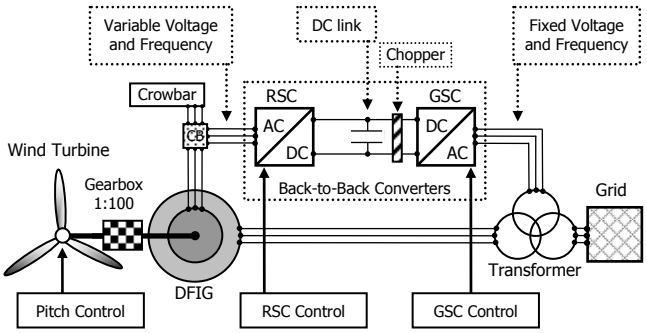

Fig. 2 Doubly fed induction generator (DFIG).

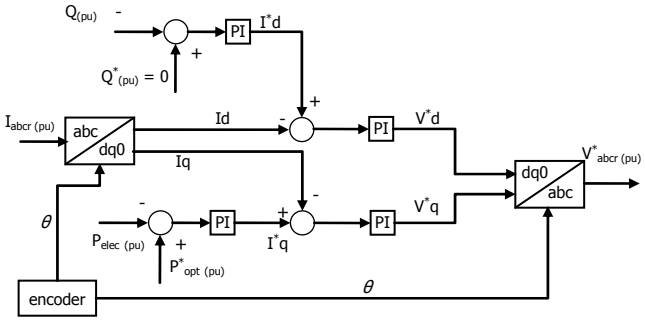

Fig. 3 RSC control diagram for DFIG in normal operation.

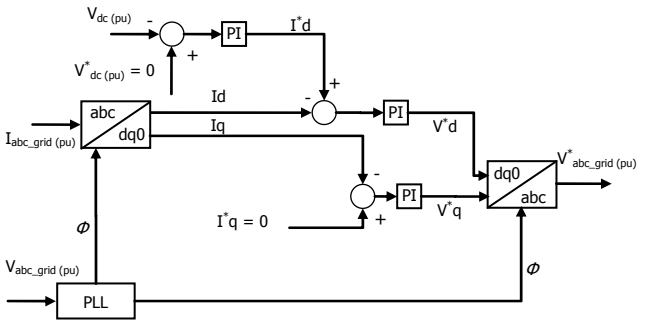

Fig. 4 GSC control diagram for DFIG in normal operation.

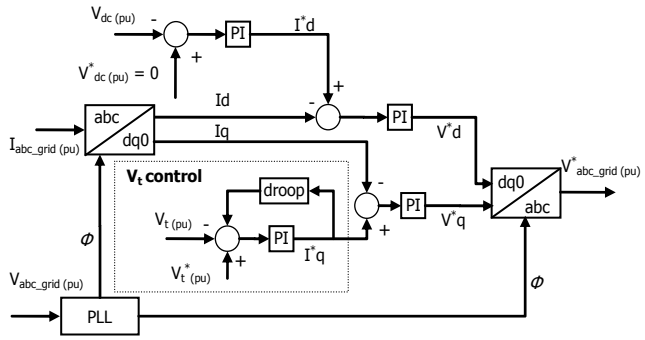

Fig. 5 GSC control diagram for DFIG in operation during fault.

As in normal operation the RSC already regulates the power factor of the DFIG, the reactive power regulation by the GSC is disable. Thus, the quadrature axis component of the reference

current is set to zero (I^*q = 0). After a dq0-to-abc transformation, the V^*d and the V^*q are sent to the PWM signal generator. Finally, V^*abc_grid are the three-phase voltages desired at the grid-side converter output. The IGBT's are considerate ideals.

C. DFIG During Grid Faults

To accomplish with new grid code requirements some methodologies have been proposed in the literature [7]-[10]. As the stator of the DFIG is connected direct to the grid, some undesirable high currents may be induced in the rotor windings and the protection system may block the RSC. Another undesirable transient is the voltage at the DC-link, which can reach high level depends on two main characteristics: low residual terminal voltage during fault and slow velocity of the RSC disconnection from the rotor winding after fault detection. These facts will contribute to make active power unbalance between RSC and GSC higher and thus, DC-link voltage level.

Depends in which TSO area that they are connected to the grid (see next section), modern wind turbines based on DFIG have to be equipped with a crowbar system and sometimes with a chopper system in order to be able to keep connected during fault. The use of a crowbar system makes the DFIG behaves like a conventional squirrel-cage induction generator expanding the rotor critical speed during the disconnection of the RSC from the rotor winding [8]. Chopper systems have been largely used on industry in application were the motor operation has a regenerative cycle (for example, old elevator systems). In wind turbine, the chopper is used to dissipate the unbalance of active power between RSC and GSC.

IV. New Grid Code Requirements

E.ON Netz is one of the German Transmission System Operators (TSO) that in its 2006 grid code [4] requires the wind farms not to disconnect during unlimited time when the voltage at the PCC drops below 80% of nominal voltage. When the PCC voltage is zero the wind farms must be connected within 150 ms. In the case of the DFIG, short term interruption (STI) is allowed with the use of protection system to not damage the converters. The Spanish grid code requirements regarding to the fault-ride through capability [5] is similar to the German, both are reproduced in Fig. 6. For voltage regulation, German grid code requires the wind farm to supply at least 1 pu of reactive current when the voltage drops below 0.5 pu. A dead band is included around the reference voltage in which the control should actuate as power factor control. They are the most restricted among the others TSO from countries with high wind power penetration.

V. Test System

The analyses are performed using the SimPowerSystems (a toolbox of Matlab/Simulink) in a modified version of the WSCC-9 Bus System (Fig. 7). This transmission system contains 9 buses (6 at 230 kV, 1 at 16.5 kV, 1 at 18 kV and 1 at 13.8 kV), 9 branches, 3 loads and 3 generators [11]. The 3 generators are adapted to represent a swing bus, a 100 MVA synchronous generator and a 164 MW wind farm.

VI. Analyses of Converter Control Strategies

The effects of three different control strategies on the grid voltage during faults are investigated in this section:

- Case A: RSC and GSC are kept in normal operation during the fault, however, RSC control is switched from constant power factor to constant voltage.
- Case B: RSC operates in the same way as in Case A and GSC controls DC-link voltage (as in normal operation) and controls the injection of reactive power.
- Case C: RSC controls only the optimum electrical power during the fault (the power factor control by RSC is deactivated) and GSC operates as well as the Case B.

A. Fault at Bus 5 cleared after 150 ms

As can be seen in Fig. 8, during this fault, the Case B corresponds to the highest level of terminal voltage. This fact can be explained since RSC controls the terminal voltage with the additional reactive power injection by the GSC (Fig. 10). The terminal voltage has the lowest value for Case C since the RSC do not participate on the reactive power control during the fault. The voltages at the DC-link (Fig. 9) are kept in acceptable limits for all the three control strategies, however, Case C has a second transient. The current of RSC in the beginning of the fault should also be monitored.

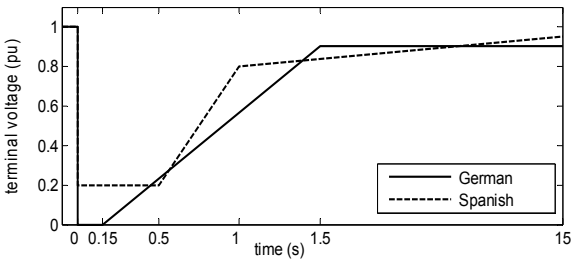

Fig. 6 Fault-ride through capability requirements.

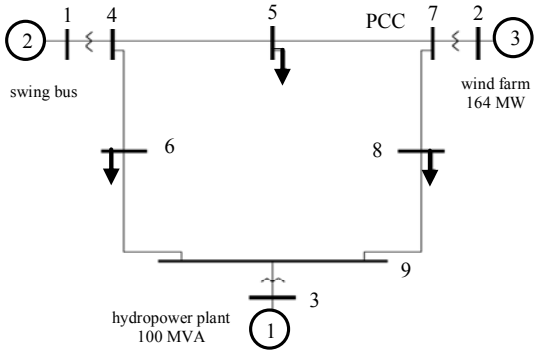

Fig. 7 Unifilar diagram of the WSCC-9 Bus System.

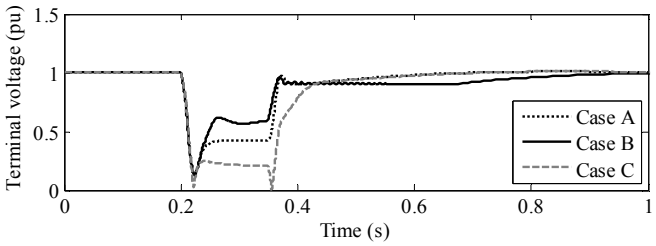

Fig. 8 Terminal voltage (Cases A, B and C).

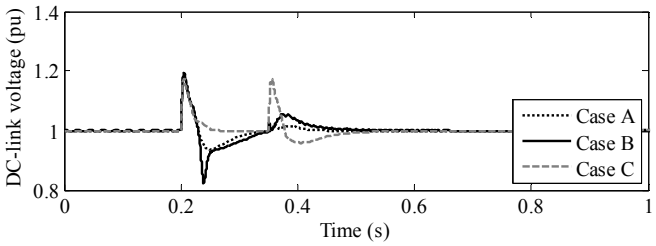

Fig. 9 DC-link voltage (Cases A, B and C).

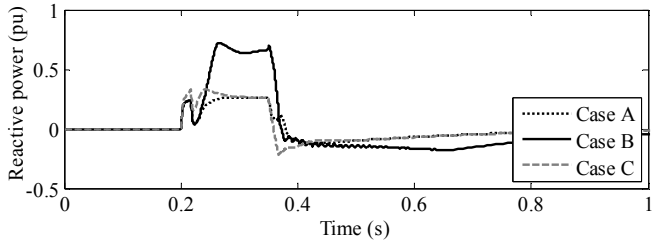

Fig. 10 Reactive power (Cases A, B and C).

B. Fault at Wind Farm Terminal cleared after 150 ms

When the fault occurs at the PCC (Bus 7) the injection of active and reactive power is limited due to low terminal voltages. The highest value of terminal voltage during the fault is when the control strategy of the Case B is used (Fig. 11). The lowest consumption of reactive power after the fault clearance is also performed by the control of the Case B (Fig. 13). The DC-link voltage has reached around 2 pu for all the three control strategies (Fig. 12) and the RSC currents has reached around 3 pu (not shown). During severe grid faults, the DFIG is not able to keep connected to the grid without some protective strategies. The use of a crowbar system will be investigated in the next section.

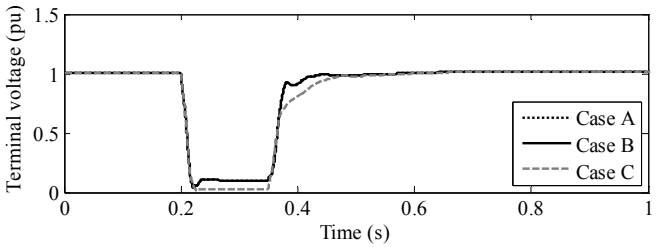

Fig. 11 Terminal voltage (Cases A, B and C).

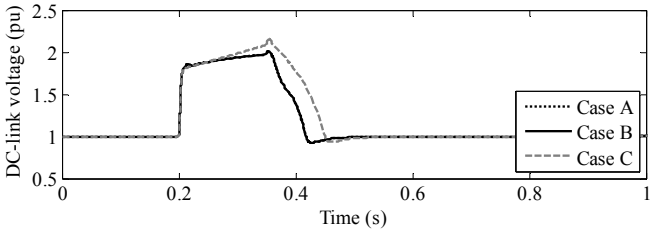

Fig. 12 DC link voltage (Cases A, B and C).

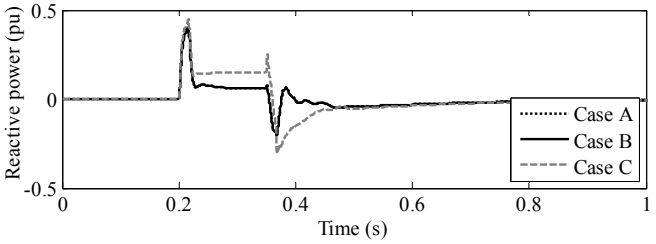

Fig. 13 Reactive power (Cases A, B and C).

VII. Analyses of Converter Protection Strategies

The effects of three different protective strategies of the back-to-back converter during faults are investigated:

- Case D: RSC is blocked and a crowbar system is activated. GSC controls reactive power during the fault and DC-link voltage. RSC is restarted and crowbar protection is removed after 200 ms.
- Case E: RSC and GSC operate in the same way as the Case D. However, RSC is restarted and crowbar protection is removed after 100 ms.
- Case F: this case is set similar to Case E, except for the addition of the DC-chopper protection. The control of the DC-chopper is activated when the DC-link voltage reaches 1.1 pu and is deactivated when reaches 1.05 pu.

A. Fault at Bus 5 cleared after 150 ms

In Fig. 14, one can see that the voltage level for cases D, E and F are maintained around 30% during the fault and they are not as effective as Cases A (around 42 %) or B (around 57 %). For Case D, after the fault clearance, the RSC is not immediately restarted, and the voltage during this period is around 0.9 pu. The RSC is restarted 50 ms after the fault clearance and finally the voltage returns to the nominal value. Considering that the period of overcurrent on the rotor winding and overvoltage on the DC-link last for a very short time, the RSC can be restarted in a period shorter than 200 ms. Thus, in Case E, the RSC is restarted 100 ms after the fault occurrence, after this period the voltage level rises, even during the fault. The use of the DC-chopper protection does not influence the terminal voltage during the fault, it is identical to Case F. The DC-chopper decreases the overvoltage at DC-link and dissipates the unbalance active power between RSC and GSC, as can be seen at Fig. 15.

In Fig. 16, Cases D, E and F inject reactive power on the grid during fault. After 100 ms, Cases E and F have the RSC restarted and then are able to inject more reactive power before the fault clearance. This fact increases the voltage level at the wind farm terminals and reduces the reactive power injection smoothly after the fault clearance. On the other hand, Case D consumes reactive power until the RSC is restarted 50 ms after the fault clearance. Evaluation of different deactivation times for the crowbar system has shown that the shorter this time is the better the voltage support during the fault.

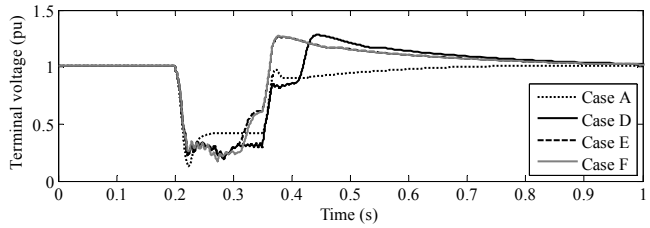

Fig. 14 Terminal voltage (Cases A, D, E and F).

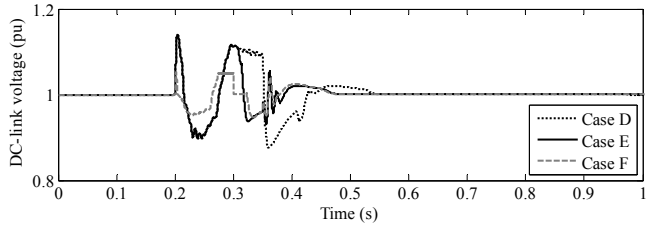

Fig. 15 DC-link voltage (Cases D, E and F).

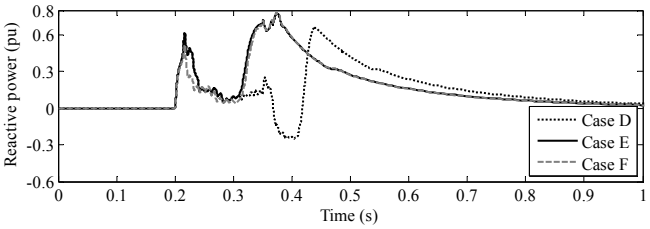

Fig. 16 Reactive power (Cases D, E and F).

B. Fault at Wind Farm Terminals cleared after 150 ms

The fault at wind farm terminal (at Bus 7) allows evaluating the DFIG voltage support in severe conditions. In Fig. 17, the terminal voltage is presented for cases D, E and F. During the fault the three cases have similar behavior, except when the RSC is restarted before the fault clearance. For cases E and F, when the RSC is restarted, terminal voltage has a slight increase during the last 50 ms of the fault. For these cases as soon as the fault is cleared the voltage returns to the nominal value. On the other hand, for case D, even after the fault clearance, while the RSC is not restarted, the voltage does not return to its nominal value and consumes reactive power in this period. The crowbar system has limited influence over the DC-link voltage. As can be seen in Fig. 18, the DC-link is kept in reasonable values only with the use of DC-chopper (Case F).

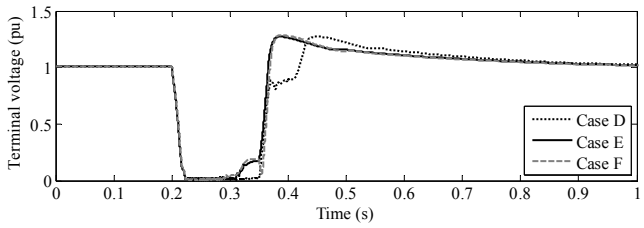

Fig. 17 Terminal voltage (Cases D, E and F).

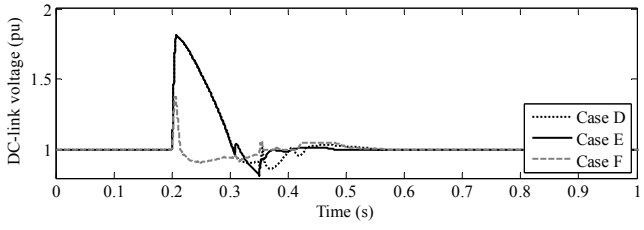

Fig. 18 DC-link voltage (Cases D, E and F).

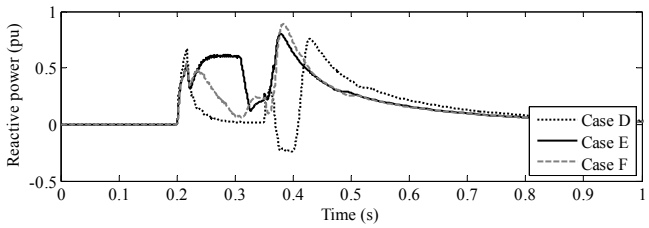

Fig. 19 Reactive power (Cases D, E and F).

VIII. CONCLUSIONS

This paper presents the dynamic model and the analysis of a DFIG-based wind farm connected to a transmission system. Three different converter control as well as three protection strategies have been analyzed during grid fault. Based on the presented results, the choice of converter control and protection strategies is related direct to the grid code requirements. Considering only that the wind turbines should keep connected during faults the crowbar system could be used during the total fault period. For more strict grid codes (such as from Germany and Spain) where the injection of reactive power is mandatory, the use of the DC-chopper turns possible the reactive power injection during the fault. In this case, also the control of reactive power by RSC and GSC is recommended and the strategy implemented in the Case F should be used.

ACKNOWLEDGMENT

The authors gratefully acknowledge the financial support from the Brazilian government via FAPESP (State of São Paulo Research Foundation), CNPq (National Counsel of Technological and Scientific Development) and CAPES ("Coordenação de Aperfeiçoamento de Pessoal de Nível Superior", in Portuguese) as well as from Germany via DAAD (German Academic Exchange Service) to develop this research.

REFERENCES

[1] H. Li, Z. Chen, "Overview of Different Wind Generator Systems and their Comparisons", IET Renewable Power Generation, vol. 2, no. 2, pp. 123–138, 2008.

[2] J. Morren, S.W.H de Haan, "Ridethrough of Wind Turbines with Doubly-fed Induction Generator During a Voltage Dip", IEEE Transactions on Energy Conversion, vol. 20, no. 2, pp. 435-441, 2005.

[3] N.R. Ullah, T. Thiringer, D. Karlsson, "Voltage and Transient Stability Support by Wind Farms Complying With the E.ON Netz Grid Code", IEEE Transactions on Power Systems, vol. 22, no. 4, pp. 1647-1656, 2007.

[4] Grid Code: High and Extra High Voltage, E.ON Netz GmbH Tech. Rep., Status: 1, 2006.

[5] P.O. 12.3 "Requisitos de Respuesta frente a Huecos de Tensión de las Instalaciones Eólicas" (in Spanish), BOE no. 254, pp. 37017-37019, October 24th 2006.

[6] J. G. Slootweg; H. Polinder; W. L. Kling, "Representing Wind Turbine Electrical Generating Systems in Fundamental Frequency Simulations", IEEE Transactions on Energy Conversion, vol. 18, no.4, pp. 516–524, 2003.

[7] V. Akhmatov, "Analysis of Dynamic Behaviour of Electric Power Systems with Large Amount of Wind Power", Ph.D. thesis, Technical Univ. of Denmark, Lyngby, Denmark, 2003.

[8] A. P. Grilo, A. A. Mota, L. T. M. Mota, W. Freitas, "An Analytical Method for Analysis of Large-Disturbance Stability of Induction Generators", *IEEE Transactions on Power Systems*, v. 22, p. 1861-1869, 2007.

[9] Mustafa Kayıkc¸ı and Jovica V. Milanovi´c, "Reactive Power Control Strategies for DFIG-Based Plants", IEEE Transactions on Energy Conversion, vol. 22, no. 2, 2007.

[10] I. Erlich, M. Wilch and C. Feles, "Reactive Power Generation by DFIG Based Wind Farm with AC Grid Connection", *12th European Conference on Power Electronics and Applications – EPE 2007*, Aalborg, 2007.

[11] P. W. Sauer and M.A. Pai, Power System Dynamics and Stability, Prentice Hall, Upper Saddle River, NJ, 1998.

BIOGRAPHIES

Maurício B. C. Salles received the degree in Electrical Engineering at Mackenzie Presbyterian University (in 1998) and a master degree from the University of Campinas – UNICAMP (in 2004). He is a Ph.D. student at the University of São Paulo – USP and has attended to an 18 months sandwich program with the Institute of Electrical Machines of RWTH Aachen University, Germany. He has experience on computational modeling of power systems and also of electromagnetic devices using the Finite Element Method. Main interests are on distributed generation, power generation, dynamics and stability of power systems, wind turbines and induction generator. He is student member of the IEEE.

José Roberto Cardoso received the B.Sc., M.Sc., Ph.D., and LivDoc degrees from the Escola Politécnica da Universidade de São Paulo (EPUSP), São Paulo, Brazil, in 1974, 1979, 1985, and 1993, respectively. In 1975, he joined the Department of Electrical Engineering, EPUSP, as an Assistant Professor. He was promoted to Doctor Professor and Associate Professor in 1985 and 1993, respectively. He was an Invited Researcher at the Grenoble Electrotechnical Laboratory, France, from 1987 until 1988, when he founded the Applied Electromagnetism Laboratory, EPUSP. He was the Chairman of COMPUMAG'97, which is the 11th Conference on the Computation of Electromagnetic Fields, in Rio de Janeiro, Brazil, in 1997. Currently, he is the Vice-Director of the EPUSP and the Head of the Applied Electromagnetism Laboratory – LMAG at PEA-EPUSP. He is member of the IEEE.

Ahda P. Grilo received the B.Sc. degree in Electrical Engineering from State University of Western Paraná (UNIOESTE) in 2003, and her M.Sc. and her Ph.D. degree in Electrical Engineering from the State University of Campinas (UNICAMP) in 2005 and 2008. She is currently an Assistant Professor at UFABC, Santo Andre, Brazil. Her interests include operation of electric power systems and distributed generation. She is member of the IEEE.

Claudia Rahmann received the degree in Electrical Engineering from University of Chile in 2005. She is presently Ph.D. student at the Institute of Power Systems and Power Economics (IAEW), RWTH Aachen University, Aachen, Germany. Her main interests are electrical power systems, power systems dynamics and stability, distributed generation, and integration of wind power into power networks.

Kay Hameyer received his PhD from the University of Technology Berlin, Germany, 1992. From 1986 to 1988 he worked with the Robert Bosch GmbH in Stuttgart, Germany, as a design engineer for permanent magnet servo motors. In 1988 he became a member of the staff at the University of Technology Berlin, Germany. Until 2004, he was professor of numerical field computation and electrical machines with the K.U. Leuven and a senior researcher with the FWO-V in Belgium, teaching CAD in electrical engineering and electrical machines. Currently, he is Head of the Institute of Electrical Machines of RWTH Aachen University, Germany. His research interests are numerical field computation, the design of electrical machines, in particular permanent magnet excited machines, induction machines and numerical optimization strategies. Prof. Hameyer is a member of the International Compumag Society and senior member of the IEEE.